to make sure that the observed dimming of type Ia SNe with z is not caused by evolution, which has been the downfall of all standard candles to date, nor by grey dust.

We can test this proposition by conducting an intense optical and IR study of a dozen type Ia SNe at $z = 0.5$, the redshift at which the acceleration of the universe was derived. As we have demonstrated with SN Beethoven, the VLT, with ISAAC and the two FORS instruments, is well suited to contribute significantly to this necessary work.

Both groups of observers are now regularly finding SNe at redshifts of order one, and with instruments like VIMOS on UT3 becoming available soon, the number of such SNe will increase. With VIMOS, it will also be possible to detect lensed (highly magnified) SNe at even higher redshifts.

At $z \approx 0.5$, type Ia SNe can only be used to place joint limits on Ω_M and Ω_Λ. They cannot be used to test whether or not the universe is flat. However, with a relatively small sample of SNe at $z \approx 1$, one can very significantly improve the determination of Ω_M and Ω_Λ separately and of the equation of state of the dark energy.

However, follow-up observations of type Ia SNe at $z \approx 1$ are both difficult and time consuming. At these redshifts, the restframe B-band, where the lightcurve of type Ia SNe are best understood, is shifted into the near-IR, where the sky background from the ground is relatively high. The R-band, where the background is more favourable, corresponds to restframe U. But observations of nearby type Ia SNe in the restframe U-band are scarce and their properties in that band are not yet accurately known. It is not clear, at present, whether from U band observations alone type Ia SNe can be used as distance indicators.

SN Beethoven, at a redshift of $z = 0.54$ and SN 1999Q at a redshift of $z = 0.46$ (Riess et al. 2000) have both been successfully observed with state-of-the-art infrared instrumentation on the largest telescopes. Near-IR follow-up observations of type Ia SNe at $z \approx 1$ and beyond will probably have to wait for the next generation of IR instruments that use adaptive optics, like NAOS and CONICA, which will be installed on the VLT next year.

In the meantime, the VLT will continue to be used to confirm and follow up type Ia SNe at more moderate redshifts, $z \approx 0.8$. Its performance will be strengthened further if the planned upgrade of FORS2 with red sensitive CCDs goes ahead.

4. Acknowledgements

The authors thank Peter Nugent, Bruno Leibundgut and Jason Spyromilio for their critical review of the manuscript.

References

Perlmutter et al. 1995, in Thermonuclear Supernovae, ed. P. Ruiz-Lapuente, R. Canal & J. Isern (NATO ASO ser. C, 486) (Dordrecht: Kluwer), 749.
Perlmutter et al. 1999, *ApJ,* **517**, 565.
Riess et al. 1998, *AJ,* **116**, 1009.
Riess et al. 2000, *ApJ,* **536**, 62.

Lensed Quasars: A Matter of Resolution

F. COURBIN[1], C. LIDMAN[2], I. BURUD[3], J. HJORTH[4], P. MAGAIN[3], G. GOLSE[5], F. CASTANDER[5]

[1]Pontificia Universidad Católica de Chile, Departamento de Astronomía y Astrofísica, Santiago, Chile
[2]European Southern Observatory, Santiago, Chile; [3]Institut d'Astrophysique de Liège, Liège, Belgium
[4]Astronomical Observatory, University of Copenhagen, Copenhagen, Denmark
[5]Laboratoire d'Astrophysique, Observatoire Midi-Pyrénées, Toulouse, France

1. Lensed Quasars

The interest in studying lensed quasars amongst the astronomical community has always been somewhat fluctuating. Periods of great enthusiasm and of profound disappointment have regularly followed one another.

Precisely described in the context of Einstein's Theory of General Relativity, the phenomenon of light deflection was first seen as a pure theoretical curiosity. It was however observed by Dyson et al. (1920), who measured, during a total solar eclipse, the angular displacement of a star by the sun's gravitational field. Gravitational lensing was thus established as an observed phenomenon, but the next important observational step was not made until 1979, with the discovery by Walsh et al. of the first lensed quasar, which had an angular separation of 6 arcsec between the two components. On the theoretical side, Refsdal (1964) proposed, well before Walsh's discovery, to use multiply imaged quasars to constrain cosmological parameters. As the travel times of photons along the light path to each quasar image are different, an intrinsic intensity variation of the quasar is seen at different moments in each lensed image. The so-called time delay between the detection of the intensity variation in each image is directly related to the cosmological parameter, H_0 and to the position and shape of the deflecting mass. One can therefore infer an estimate of H_0 by measuring the time delay, provided the gravitational potential responsible for light splitting is known. Conversely, one might as well want to assume a "preferred" value for H_0 and use the time delay to constrain a lens model, i.e., to study the mass distribution in distant lens galaxies. Both issues are undoubtedly of capital importance. They both require high spatial resolution observations. With the Hubble Space Telescope (HST) or, better, with large ground-based telescopes located in privileged sites, it is now possible to perform in a routine manner observations which were impossible only 10 years ago. As an illustration of this, we present in this report recent VLT FORS2 observations of HE 1104-1805, a doubly imaged quasar at z = 2.319 discovered in the framework of the Hamburg-ESO survey for bright quasars (Wisotzki et al. 1993). The choice of HE 1104-1805 is not intended to be representative of the importance of this particular object, but rather reflects how old observationally intractable problems can be tackled in a new way. We also present more recent results, obtained at the 1.54-m Danish telescope for another Hamburg-ESO quasar: HE 2149-2745.

2. The First Step: The Lens Geometry and the Time Delay

Resolving the blended images of multiply imaged quasars is one way to confirm or rule out their lensed nature.

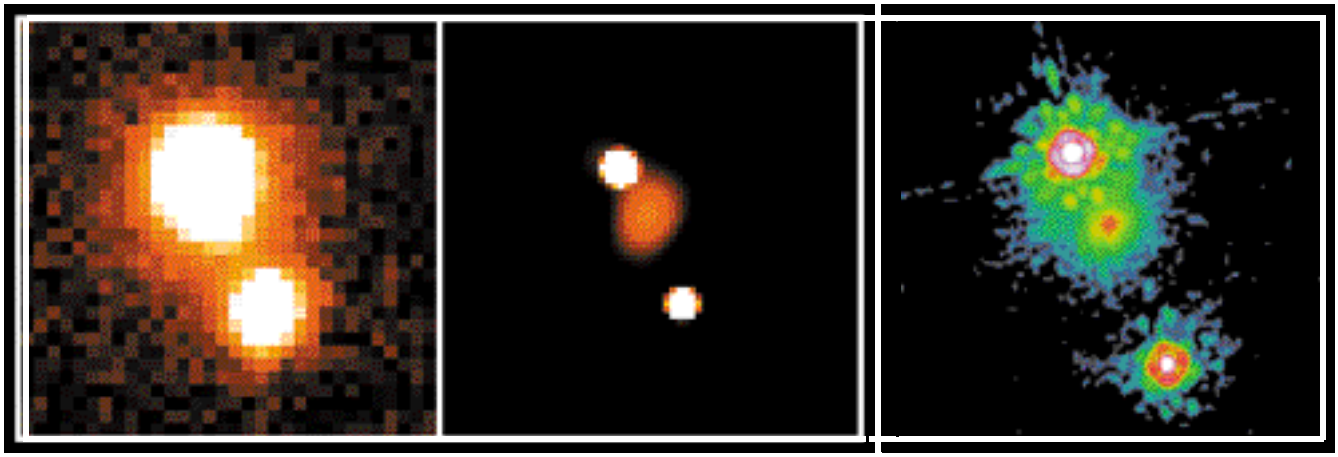

Figure 1: A J-band image of HE 1104-1805 obtained at the ESO/MPI 2.2-m telescope with IRAC2b (Courbin et al., 1998). The seeing is about 0.8 arcsec and the pixel size is 0.28 arcsec. The middle panel shows a deconvolved version of the image, with a resolution (FWHM) of 0.28 arcsec and clearly revealing the lensing galaxy. An HST H-band image obtained later (PI: Emilio Falco) is displayed on the right panel and confirms the ground-based observation.

If each component of a system shows the same colour, or even better the same spectral energy distribution, the quasar has a good chance of being lensed. However, dust along the line of sight, microlensing, and even intrinsic variability of the quasar can affect the spectral energy distribution of the components. Finding the faint lensing galaxy between the quasar images is a much more reliable criterion. We show in Figure 1, left panel, the discovery image of the lens in HE 1104-1805 (Courbin et al. 1998). This J-band image was taken at the ESO/MPI 2.2-m with IRAC2b, which by today's standards has a relatively small field of view, 1 arc minute on a side, with coarse sampling, 0.28 arcseconds per pixel. It is difficult to see the lens in this image. However, with deconvolution (Magain et al. 1998; MCS) it can be detected at a distance of 1 arcsec from the bright quasar image (Fig. 1, middle). The HST-NICMOS2 image obtained by Lehar et al. 2000 in the H-band is also displayed (Fig. 1, right). Comparison with the deconvolved image confirms not only the position of the lens, but also its ellipticity and orientation. The seeing at the time the data were taken was 0.8″, which is average for La Silla. With more modern instrumentation and larger telescopes one can do better. On Paranal, the seeing is often better that 0.5″ and the pixel scale of modern detectors is usually of the order of 0.1″.

The measurement of the time delay itself remains challenging. Precise light curves with good temporal sampling have to be obtained for each component. It can take several years of continuous monitoring to obtain the time delay of a single lens. HE 1104-1805 was spectrophotometrically monitored at ESO for four years by Wisotzki et al. (1998), and the time delay was estimated to be 0.73 years. We are currently using the Danish 1.54-m and the 3.5-m NTT to monitor on a weekly basis almost all multiply imaged quasars visible from the Southern Hemisphere (PI: P. Magain for ESO time, J. Hjorth for Danish time).

The image quality is usually between 0.8 and 1.5 arcsec, which, with deconvolution, still allows accurate photometry of objects with angular separations of less than 1 arcsec, down to R ~ 19–20. One of the first results from this monitoring, the light curve for HE 2149-2745 (Lopez et al. 1998) is shown in Figure 2 (Burud et al. 2001). In this case, the two images of the quasar at z = 2.03 are separated by 1.7 arcsec.

The monitoring data of HE 2149-2745 have been obtained during a wide variety of observing conditions, even during full moon or through thin cirrus, and very few epochs have been missed. Loosing too many data points due to instrument scheduling or to excessively restrictive observing constraints would be fatal. Therefore, all available data have been used, even those taken under poor conditions.

We would like to point out that none of this would have been possible without the excellent collaboration of the 2.2-m and NTT teams and of the large number of visiting astronomers who performed observations for this programme. We are extremely grateful to all these people.

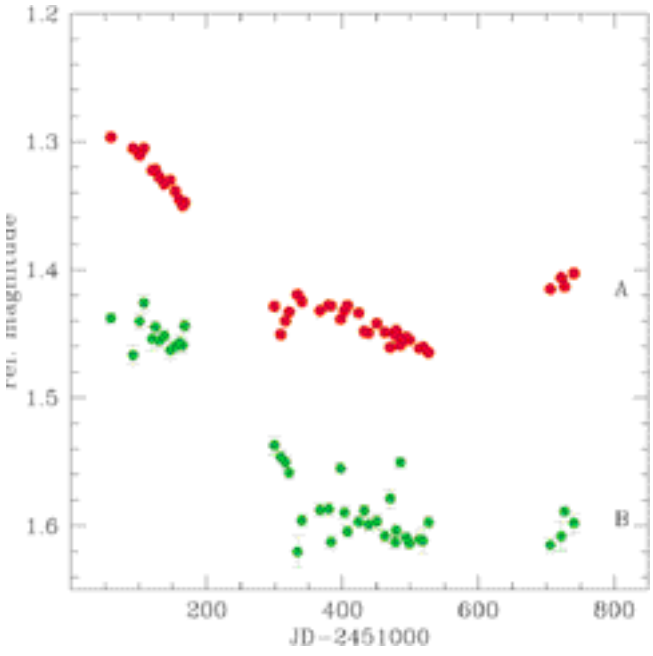

Figure 2: Example of light curve obtained at ESO in the framework of the lens monitoring programme. These light curves, for the two quasar images of HE 2149-2745 (Burud et al., 2001) have been constructed from data obtained at the 1.54-m Danish telescope under average weather conditions. The red curve shows the variation of the brightest quasar image while the green one corresponds to the fainter component, heavily blended with the lensing galaxy. The shift in time between the curves is the time delay. The present data suggest a very rough estimate of ~ 100 days. Future monitoring will provide a better measurement of the delay.

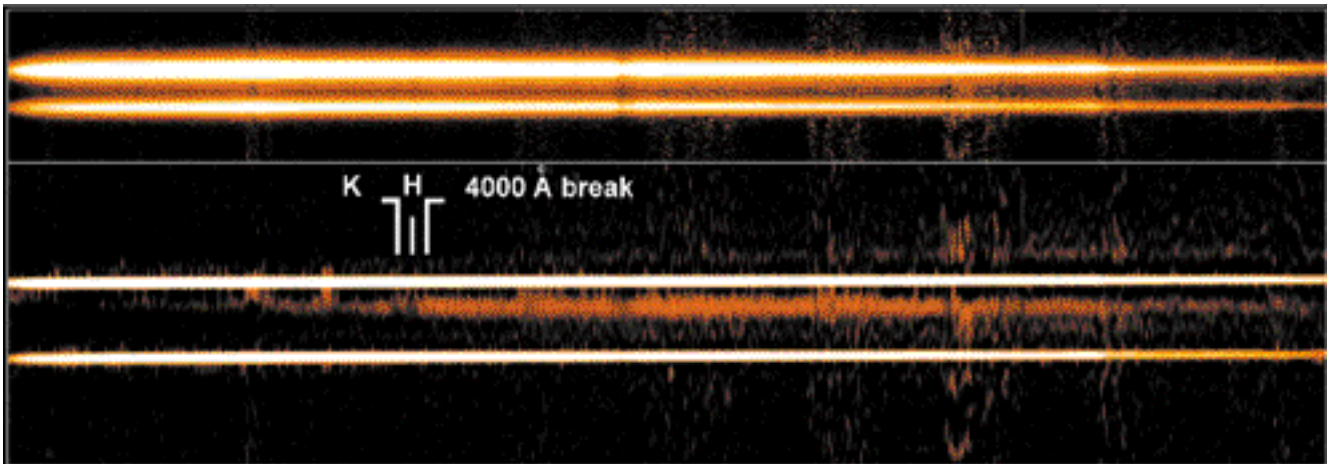

Figure 3: The two-dimensional spectrum of HE 1104-1805 (Lidman et al., 2000). The image at the top is the spectrum of the lens after bias subtraction, flat fielding, and sky subtraction, with the 2 quasar spectra separated by 3.14 arcsec. The image at the bottom is the spatially deconvolved spectrum, with a (spatial) pixel size twice as small as in the original data (this is why the height of the deconvolved spectrum is twice that of the raw spectrum). The lens galaxy, including the H and K bands and the 4000Å break, is clearly visible. The spatial resolution in this spectrum is 0.2 arcsec.

3. A Second, More Challenging Step: Spectroscopy of the Lens

Imaging the lensing galaxy is difficult, but obtaining its spectrum is even more so. Accurate modelling was therefore often hampered by the lack of the lens redshift. Lens galaxies are heavily blended with the bright quasar images and are often too faint for the HST. The solution to the problem might be, here again, to use good-quality ground-based data. Using the spectroscopic version of the MCS deconvolution (Courbin et al. 2000a, Courbin et al. 1999) and VLT data, we have obtained a spectrum of the lensing galaxy in HE 1104-1805 (Lidman et al. 2000) and determined its redshift.

Apart from the many unpublished attempts to measure it, the redshift of the lens had been estimated from indirect means. From IR and optical photometry, Courbin et al. (2000b) estimated a redshift in the range z = 0.8 to z = 1.2. From the time delay measured at the ESO 3.6-m and a model of the lens, Wisotzki et al. (1998) estimated a redshift of z = 0.79 and from the position of the lens on the fundamental plane, Kochanek et al. (2000) gave a redshift of z = 0.73.

Given these redshift estimates, a deep spectrum in the optical was likely to settle the issue. The VLT spectroscopic observations were taken with FORS2 on Kueyen at the Cerro Paranal Observatory on April 1, 2000 as part of ESO programme 65.0-0566(A). The observations consisted of three 1080-second exposures with the G200I grism and the high-resolution collimator.

This gives a scale of 0.1″ per pixel in the spatial direction, which is excellent for deconvolution purposes. The corresponding scale in the spectral direction is approximately 4Å per pixel. The observing conditions were clear and the external seeing varied between 0.5″ and 0.9″.

We used the movable slits in the FORS2 focal plane to select targets and set the slit width. One slit was placed on the lens and aligned along the two components, three slits were placed on field stars that were used to determine the PSF for the deconvolution and to correct for telluric absorption, one slit was placed on a random object and the remaining slits were closed. Indeed, the final configuration

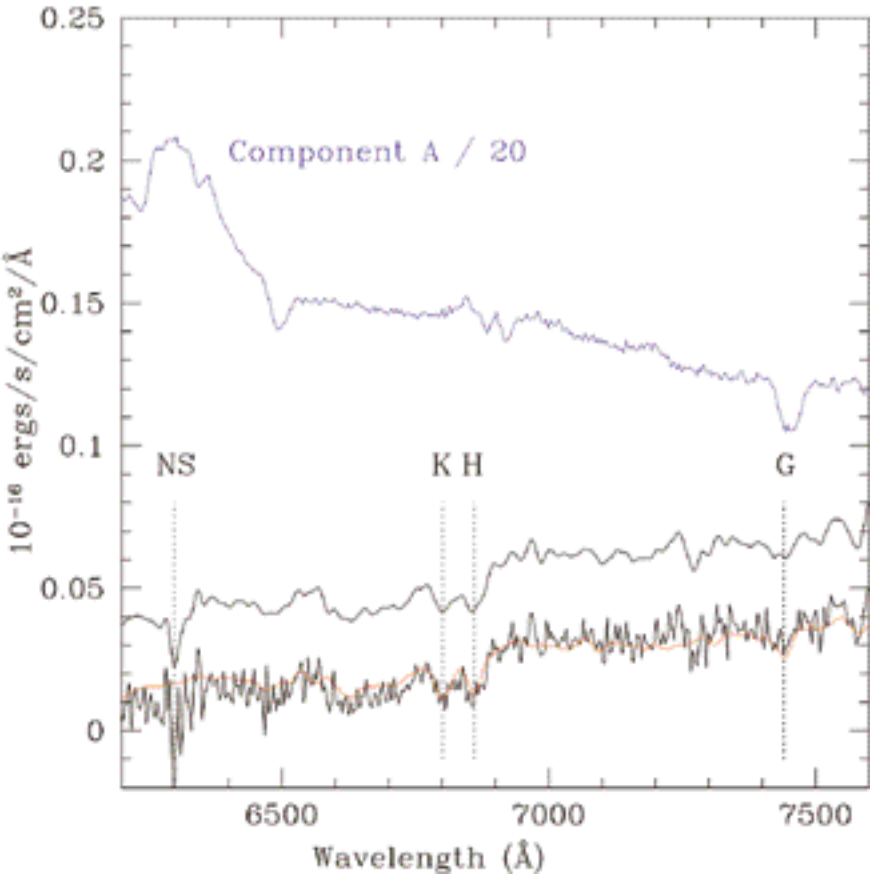

Figure 4: The spectrum of the lens in HE 1104-1805 (bottom). The major absorption lines are identified with the vertical dashed lines. Also plotted, but at 1/20th of the scale, is component A of the quasar (top). The red line is a template of an elliptical galaxy shifted to z = 0.729 and not a smoothed version of the spectrum. The smoothed version of the spectrum has been shifted vertically by 0.03 units for clarity. The H and K Calcium bands and the G band are indicated. A strong sky line at about 6300 Å and introducing significant noise is also indicated.

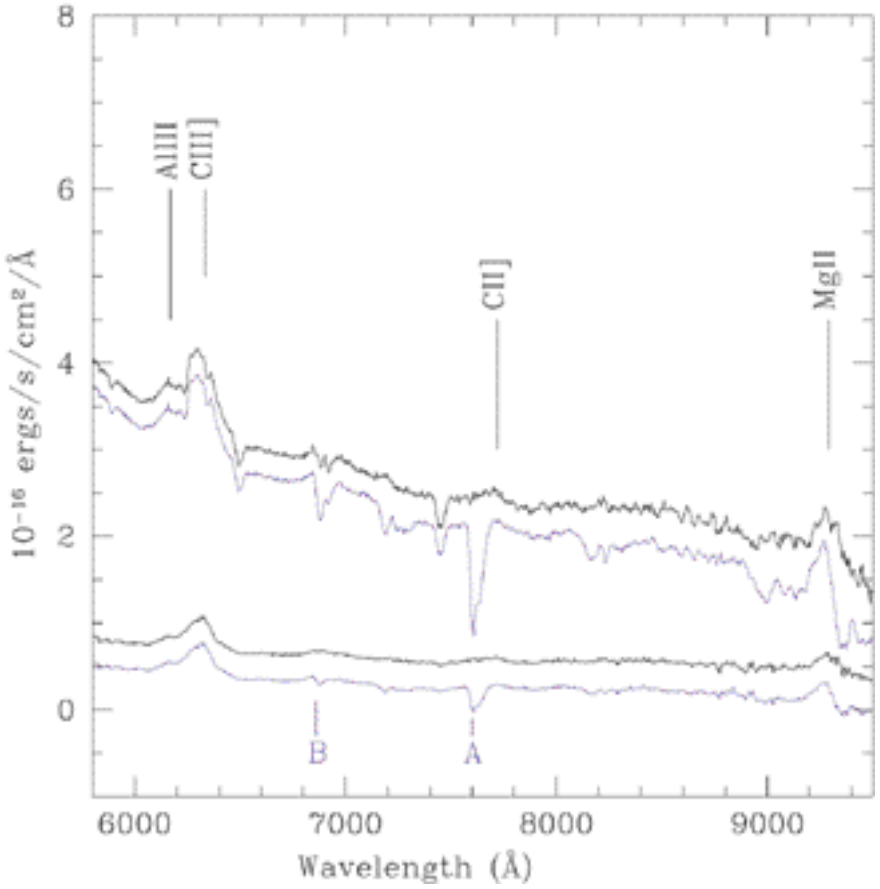

Figure 5: One-dimensional spectra of components A and B of HE 1104-1805. The blue lines are the spectra before the correction for telluric features was applied and the black lines are the spectra after the correction. For clarity, the blue lines have been shifted down by 0.3 units.

looks very similar to the configuration presented in right hand side of Figure 1 of Courbin et al. (1999).

The lensing galaxy is four to five magnitudes fainter than component A, which is located only one arc second away. Even with good seeing, the light of the galaxy is heavily blended with that of the quasar. To detect the lensing galaxy, extract its spectrum and measure the redshift, deconvolution in the spatial direction was essential.

The 2-D spectrum of the lens is shown in Figure 3. The lens is completely invisible in the raw data, shown in the top panel, while it is obvious, including absorption features, in the bottom panel. The 1-D extraction of the deconvolved lens spectrum is displayed in Figure 4. An unsmoothed version is shown at the bottom of the figure with a smoothed version, shifted by 0.03 units on the vertical scale. Also shown, but reduced by a factor of 20, is the spectrum of component A. Note that the lens spectrum shows no trace of contamination by the QSO emission lines. The Calcium H and K absorption lines are clearly detected in the lens and the G-band is marginally detected. A template spectrum of an elliptical galaxy shifted to z = 0.729 (Kinney et al. 1996) is overplotted in red. Cross correlation of the data with this template allows us to derive the redshift of the lens: z = 0.729 ± 0.001.

The spectra of the two components of the quasar are shown in Figure 5. We plot the spectra before and after the telluric features have been removed. The PSF stars are fainter than the quasar, so the later spectrum is noisier. The main emission features of the quasar and the telluric A and B bands are indicated in the figure.

4. On the Future of Quasar Lensing

Until recently, it was hard to resolve the lensed components of multiply imaged quasars. It is now relatively straightforward and it is becoming possible to extract the spectrum of the faint lensing galaxy. Measuring time delays is also becoming easier, since one can efficiently process data obtained with medium-size telescopes under average or poor weather conditions.

The remaining problem in using gravitational lenses for measuring the Hubble constant is now model degeneracy; several models can reproduce the available constraints for any given system. Observing many different lenses, with very different image configurations is one approach to reduce the degeneracy. Another approach is of course to improve the accuracy of the observations for each individual system. Until now, one reconstructs the mass profile of the lens by probing the gravitational potential at only 2 or 4 positions, i.e., the position of the quasar images. Systems with more images are probably extremely rare, so the only way to use more constraints is to observe the distorted images of other objects behind the lensing galaxy. The host galaxy of the lensed quasar is an obvious candidate (e.g., Kochanek et al. 2000). With the very high angular resolution soon achievable with adaptive optics (AO) systems mounted on 8-m-class telescopes, it will be possible, in many objects, to see the quasar host galaxy as a lensed ring, hence providing new constrains for the mass modelling. Advanced multi-conjugate AO systems will allow for similar resolutions but on a wider field of view (about 1 arcmin) and with good PSF quality. Small arclets, as presently observed in lower-resolution observations of rich galaxy clusters, should be seen in the immediate vicinity of the lens, providing us with measurements of the lensing potential at many positions.

It is very tempting to speculate further on what we may be doing in a few years from now. Although such an exercise is always somewhat dangerous, it is not foolish to predict that a spectrograph mounted on an AO system will allow us to measure the rotation curve of lens galaxies, making it possible to compare, for the first time, the mass derived from direct velocity curve measurement, with the mass inferred from lensing. In the longer term, one may be using 2-D spectrographs on OWL to map the velocity field of lens galaxies, lensed quasar hosts, and lensed arclets in order to derive very precise lens models which will probably be fully non-parametric (e.g., like those described by Williams & Saha, 2000).

In conclusion, leadership of ESO in the field of lensed quasars can be maintained, by using both the small telescopes to measure time delays, and the larger ones to conduct imaging/spectroscopic observations with unprecedented quality. It will be interesting to see how lensed quasars will be used in the future. Will we derive H_0 from quasar time delays, using the very detailed observations of lens galaxies, or will we use the value of H_0 derived from other techniques to infer the mass profile for distant galaxies using lensing? In either case, there is a great deal to be learnt from the study of lensed quasars.

5. Acknowledgements

It is a pleasure to thank Thomas Szeifert for his expert support on FORS2 at VLT-UT2. We also thank all

those observers – and there are many – who helped us to obtain data on the NTT and the Danish 1.54-m. We also specially thank the NTT and 2.2-m teams, whose professional and courteous support has made the monitoring programme a success. Frédéric Courbin acknowledges financial support through the Chilean grant FONDECYT/3990024. Additional support from the European Southern Observatory and through CNRS/CONICYT grant 8730 “Mirages gravitationnels avec le VLT: distribution de matière noire et contraintes cosmologiques” is also gratefully acknowledged.

References

Burud, I., et al. 2001, in preparation.
Courbin, F., Lidman, C., Magain, P. 1998, *A&A*, **330**, 57.
Courbin, F., Magain, P., Sohy, S., Lidman, C., and Meylan, G., 1999 *The Messenger,* **97**, 26.
Courbin, F., Magain, P., Kirkove, M., Sohy, S. 2000a, *ApJ,* **529**, 1136.
Courbin, F., Lidman, C., Meylan, G., Kneib, J.-P., Magain, P., 2000b, *A&A,* in press.
Dyson, F. W., Eddington, A. S., Davidson, C. R., 1920, *Mem. Roy. Astr. Soc.,* **62**, 291.
Lehar, J., Falco, E., Kochanek, C. et al. 2000, *ApJ*, **536**, 584.
Lidman, C., Courbin, F., Kneib, J.-P., et al., 2000, *A&A,* submitted.
Lopez, S., Wucknitz, O., Wisotzki, L., 1998, *A&A,* **339**, L13.
Kinney, A.L., Calzetti, D., Bohlin, R.C., et al., 1996, *ApJ,* **467**, 38.
Kochanek, C.S., Keeton, C.R., McLeod, B.A., et al. 2000, astro-ph/0006116.
Magain, P., Courbin, F., Sohy, S., 1998, *ApJ,* **494**, 472.
Refsdal, S., 1964, *MNRAS,* **128**, 295.
Walsh, D., Carswell, R. F., Weymann, R. J., 1979, *Nature,* **279**, 381.
Williams, L.L.R., Saha, P., 2000, *AJ,* **119**, 439.
Wisotzki, L., Koehler, T., Kayser, R., Reimers, D., 1993, *A&A,* **278**, L15.
Wisotzki, L., Wucknitz, O., Lopez, S., Sørensen, A., 1998, *A&A,* **339**, L73.

3D Structure and Dynamics of the Homunculus of Eta Carinae: an Application of the Fabry-Perot, ADONIS and AO Software

I. MOTIONS IN HOMUNCULUS

D. CURRIE [a], D. LE MIGNANT [a], B. SVENSSON [a], S. TORDO [c], D. BONACCINI [a]

[a]European Southern Observatory, Garching, Germany
[b]Università di Bologna, Dipartimento di Astronomia, Bologna, Italy
[c]Osservatorio Astronomico di Bologna, Bologna, Italy

Summary

Eta Carinae is an extremely massive and highly evolved member of the Carinae starburst region. It has undergone numerous eruptions over the past millennium. In 1841, a giant eruption ejected several solar masses or more of material. Most of this material is currently in the dusty nebula denoted as the “Homunculus”.

The Adaptive Optics Instrument of the ESO 3.6-m telescope, ADONIS, has been used in its Fabry-Perot interferometric mode to carry out observations of the nebula near the Brackett γ line at 2.16 μm. These observations

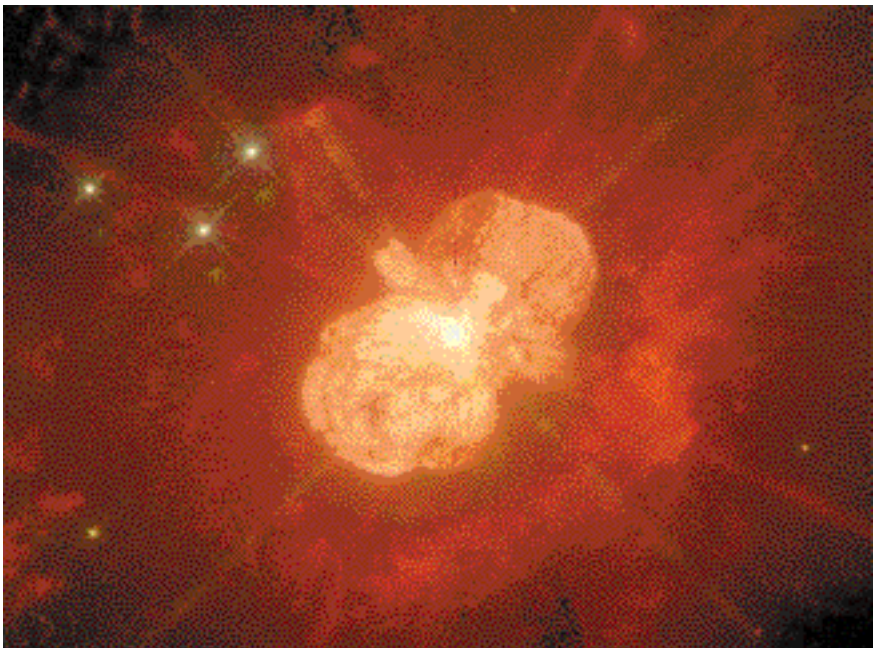

Figure 1: The Homunculus of η Carinae (i.e., the bright double-lobed structure) as observed with the WFPC2 of the Hubble Space Telescope. Data were obtained in a narrow-band filter centred at the emission line of Hα. The dynamic range of elements visible in this image is over one million. North is up, and the width of the image is about 45 arcseconds.

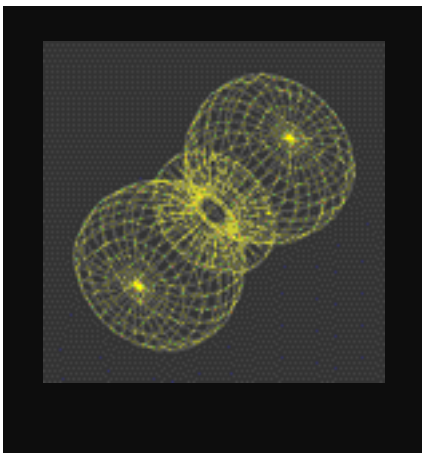

Figure 2: Three-Dimensional Representation of the Double-Flask Model[3] of the Homunculus, derived from the astrometric motion[2] and the Doppler velocities[5] of the clumps, and the assumption of rotational symmetry. This has the same scale and orientation as Figure 1.